

Electrooxidation of the calix[4]arenedihydroquinone mechanistic investigation and electrodeposition of the oxidised form on platinum grid

Oumayma Ben Youchret Zallez ·
Salma Besbes Bentati · Marcel Bouvet ·
Hechmi Said

Received: 21 December 2009 / Accepted: 8 October 2010 / Published online: 2 November 2010
© Springer Science+Business Media B.V. 2010

Abstract The electrochemical behaviour of 5,17-di-tert-butyl-11,23,25,27-di-dihydroxy-26,28-diméthoxy calix[4]-arene has been investigated at a platinum electrode in aprotic solvent by cyclic, square wave and rotating-disk voltammetry as well as by controlled potential coulometry. By comparing to the ferrocene, the height of the first irreversible transfer process involves only one-electron transfer, which corresponds to the formation of the radical cation. However, the last substance undergoes a fast chemical reaction and follows an EC_HE sequence. But, the large scale electrolysis at the first anodic peak required a consumption of 2.25 Faradays per molecule. When we interrupt the electrolysis after consumption of 1 Faraday per molecule, an intermediate compound was formed, which is the calix[4]arenequinhydrone ($X_4\text{Me}_2(\text{H}_2\text{Q})\text{Q}$) through a partial reduction of the start product. Furthermore, the reaction may evolves in solution following an EC_HEC_H redox process for generating the calix[4]arenedi-quinone ($X_4\text{Me}_2\text{Q}_2$). On the other hand, the voltammetric follow-up shows the electrogeneration to the departure product during the macroscale electrolysis according an EC_HE-disproportionation mechanism. When the electrolysis was performed after the third oxidation peak, ($X_4\text{Me}_2\text{Q}_2$) was electrogenerated in solution and was deposit, afterward, on the platinum grid.

Keywords Calix[4]arenedihydroquinone · Calix[4]arenquinhydrone · Anodic oxidation · Cyclic voltammetry · Square wave voltammetry · Electrodeposition

Introduction

The electrochemical oxidation of different calixarenes has been widely investigated in aprotic media and at several working-electrodes. Their application in the field of electrochemistry has been reviewed [1, 2]. Cyclic voltammetry (CV) of the unsubstituted calix[4]hydroquinone was studied by Suga et al. [3] in *N,N*-dimethylformamide at glassy carbon electrode. Two electron transfers have been attributed to the first anodic wave like the classic hydroquinone [4].

Morita et al. [5, 6] and Gutsche and co-workers. [7, 8] showed that the chemical oxidation of the unsubstituted phenol rings containing calix[n]arenes studied results in the formation of calix[4]arene-mono-, -di-, -tri- and tetra-quinones, depending on the number of free phenolic rings in the starting calixarenes. Recent works by Vataj et al. [9] interested to the electrochemical oxidation of calixarene diamides and confirmed that the electrooxidation of the calixhydroquinones studied generate the corresponding diquinone. However, in voltammetric studies, they showed that the apparent electron transfer [10] of the studied calixarenes could not be confirmed by coulometric measurements in macroscale electrolysis. Nevertheless, electrodeposition of phenolic derivatives was performed at a glassy carbon electrode in aprotic solvent by repetitive CVs [11].

A very simple and interesting example is the well-known quinhydrone that is a molecular complex between *p*-benzoquinone (BQ) and hydroquinone (H₂Q). Its crystal

O. B. Y. Zallez (✉) · S. B. Bentati · H. Said
Laboratoire de thermodynamique et d'électrochimie, Faculté des sciences de Bizerte, 7021 Zarzouna, Bizerte, Tunisia
e-mail: oumayma_2005@yahoo.fr

M. Bouvet
Laboratoire de Chimie Inorganique et Matériaux Moléculaires, Université Pierre et Marie Curie, CNRS-UMR 7071, 4 place Jussieu, Case courrier 42, 75252 Paris Cedex 05, France

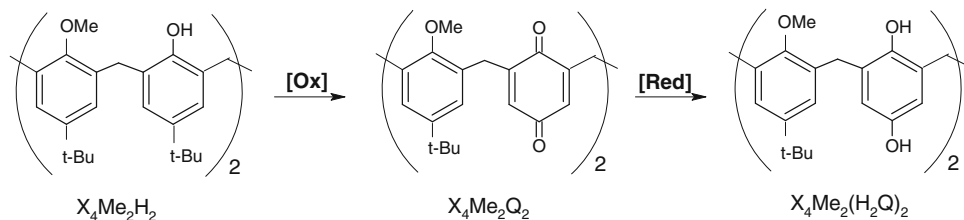
structure reveals the formation of regular alternate donor/acceptor stacks [12, 13]. The quinhydrone role was evidenced in biological systems: the quinone reductase activity of the inner-membrane protein DsbB, which is present in *Escherichia coli*, involves a quinhydrone type charge-transfer complex [14]. The family of calixarenes occupies an important place in host–guest chemistry, [15, 16] but only a few examples of calixarènes are known to accommodate neutral entities [17, 18]. The chemical reduction of the Di(methoxy-*p*-*tert*-butyl)calix[4]arenediquinone led to its calix[4]arenedihydroquinone and its partial reduction led to the calix[4]arenequinhydrone charge transfer complex [19].

In the present work, the electrochemical study of the 5,17-di-*tert*-butyl-11,23,25,27-di-dihydroxy-26,28-dimethoxy calix[4]arene $X_4\text{Me}_2(\text{H}_2\text{Q})_2$ in acetonitrile at Pt electrodes by CV square wave (SWV) and rotating-disk voltammetries are used to elucidate the mechanism of formation of the above products and to determine the standard potential E^0 of the couple cation/radical.

The preparative electrolyses demonstrate that heterogeneous oxidation of that substrate allows the synthesis of 5,17-di-*tert*-butyl-23,25-di-dihydroxy-26,28-diméthoxy calix[4]quinhydrone ($X_4\text{Me}_2(\text{H}_2\text{Q})\text{Q}$) as an intermediate product and the 5,17-di-*tert*-butyl-26,28-dimethoxycalix[4]arenediquinone ($X_4\text{Me}_2\text{Q}_2$) as a final product in aprotic media. The formed products were analysed by ^1H NMR and IR spectroscopic techniques. Mass spectroscopy analysis was used to characterize the products isolated from the electrochemical reaction. Our target molecules [19] are 5,17-di-*tert*-butyl-11,23,25,27-di-dihydroxy-26,28-diméthoxy calix[4]arène ($X_4\text{Me}_2(\text{H}_2\text{Q})_2$) (**1**), 5,17-di-*tert*-butyl-23,25-di-dihydroxy-26,28-diméthoxy calix[4]quinhydrone ($X_4\text{Me}_2(\text{H}_2\text{Q})\text{Q}$) (**2**) and 5,17-di-*tert*-butyl-26,28-diméthoxycalix[4]diquinone ($X_4\text{Me}_2\text{Q}_2$) (**3**).

The oxidation mechanism of the calix[4]dihydroquinone is of primary interest in view of the existence of an intermediate product such as calix[4]quinhydrone (diquinone-dihydroquinone pair). Taking into account that the oxidation mechanism of calix[4]dihydroquinone are under the control of acid/base reaction [20]. In some way, it could be considered that intermolecular protonation/deprotonation influence deeply the mechanism [9, 10].

Scheme 1 Schematic pathway of dimethoxycalix[4]arenedihydroquinone $X_4\text{Me}_2(\text{H}_2\text{Q})_2$ **1** electrooxidation



Experimental

Tetrabutylammonium perchlorate TBAP (Fluka) was used as supporting electrolyte. The acetonitrile 99% was purchased from Acros organics and was used as received.

The synthesis of 5,17-di-*tert*-butyl-11,23,25,27-di-dihydroxy-26,28-diméthoxy calix[4]arène $X_4\text{Me}_2(\text{H}_2\text{Q})_2$ (**1**) were carried out under argon using Schlenk tube techniques and dichloromethane were distilled before use from over CaH_2 under argon. Trifluoroacetic acid and thallium (III) trifluoroacetate were purchase from Strem Chemicals Alfa-Aesar, respectively, and used as received. NaBH_4 (Acros) and NaH were used as received. Using the methodology developed by McKillop et al. [21] we synthesized from dimethoxycalix[4]arene $X_4\text{Me}_2\text{H}_2$ [22], the dimethoxycalix[4]arenediquinone $X_4\text{Me}_2\text{Q}_2$ as described by Beer et al. [23]. On reduction of dimethoxycalix[4]arenediquinone by NaBH_4 we synthesized the corresponding dimethoxycalix[4]arenedihydroquinone **1** [24] as white powder (Scheme 1). **1** was considered as the starting product for the present electrochemical studies.

The electrochemical set-up consisted of a Tacussel (PGP 201) potentiostat. A three-electrode cell with compartments separated by a porous glass was used. The working electrode was a platinum disc electrode ($\phi = 2 \text{ mm}$) (EDI type Radiometer) and a platinum wire as counter electrode. The reference electrode (saturated calomel electrode, SCE) was separated from the bulk solution by a sintered-glass bridge filled with the solvent and the supporting electrolyte.

Prior to each measurement, the working electrode was polished with a set of fine alumina powders. All the experiments were carried out at laboratory temperature.

Solutions containing TBAP 0.1 M as supporting electrolyte were protected from atmosphere with argon prior to each cyclic voltammetry measurement and the gas flow maintained during the CV experiments.

An Autolab potentiostat/galvanostat PGSTAT 30 assisted by GPES electrochemical software was used for macroelectrolysis and square wave voltammetry (SWV) measurements.

Macrocyclic electrolysis of **1** was carried out under argon atmosphere in a separated cell. The separation was realized with a sintered glass (porosity number 4). An 8 cm²

platinum grid was used as working electrode and a 2.5 cm^2 platinum grid was used as counter electrode. SWV were realized in the potential range 0.5–2.4 V, with frequency (f) of 10 s^{-1} , pulse amplitude (ΔE_p) of 25 mV, step potential (ΔE_S) of 20 mV and equilibration time of 5 s.

^1H NMR analyses were recorded with a Bruker 300 MHz. ATR diamond was used as characterization technique of spectroscopy IR and was performed with a BRUKER TENSOR 27 spectrometer. The MALDI-TOF mass spectrum was achieved by a UPMC-LCSOB apparatus in a HCCA (α CYANO-4-HYDROXY) as a matrix.

Electrochemical synthesis of 5,17-di-tert-butyl-23,25-dihydroxy-26,28-diméthoxy calix[4]quinhydronne ($X_4\text{Me}_2(\text{H}_2\text{Q})\text{Q}$) (2) and 5,17-di-tert-butyl-26,28-diméthoxycalix[4]diquinone ($X_4\text{Me}_2\text{Q}_2$) (3). A 0.1 M TBAP solution of **1** (46.5 mg; 0.078 mmol) was electrolysed at a potential of 1.3 V versus SCE. Electrolysis was stopped after a consumption of 1 electron per molecule. After evaporation of the solvent, the crude material was extracted with diethyl ether and purified on column chromatography (silica gel 60, $\text{CH}_2\text{Cl}_2\text{-(CH}_3)_2\text{CO}$, 95/5, v/v). The obtained products were separated by chromatography on preparative patches of silica gel (eluent: $\text{CH}_2\text{Cl}_2\text{-(CH}_3)_2\text{CO}$, 95/10, v/v) to give **2** (10 mg; yield: 21.5%) and **3** (12 mg; yield: 25.8%), additionally to starting material **1** (11 mg; yield: 23.6%). The yield was calculated as the ratio $m_{\text{product}}/m_{\text{initial substrate}}$.

Compound 2: TLC (SiO_2 , eluent $\text{CH}_2\text{Cl}_2\text{-(CH}_3)_2\text{CO}$, 90/10, v/v) $R_f = 0.59$; MALDI-TOF MS: m/z 594 (M^+); 616 ($\text{M} + \text{Na}^+$); 633 ($\text{M} + \text{K}^+$). IR (KBr) 1655, 1604, 1490, 1300, 1207, 1013 cm^{-1} . ^1H NMR (300 Hz, CD_3CN): δ (ppm) 1.17 [s, 9H, $\text{C}(\text{CH}_3)_3$]; 3.31 (d, $J = 13$ Hz, 1H, ArCH_2Ar), 3.93 (s, 6H, OCH_3), 4.22 (d, $J = 13$ Hz, 1H, ArCH_2Ar), 6.20 (s, 2H, OH), 6.60 (s, 4H, ArH), 7.15 (s, 4H, ArH), 7.74 (s, 2H, OH).

Compound 3: TLC (SiO_2 , eluent $\text{CH}_2\text{Cl}_2\text{-(CH}_3)_2\text{CO}$, 90/10, v/v) $R_f = 0.85$; MALDI-TOF MS: m/z 594.39 ($\text{M} + 2\text{H}^+$); 615.37 ($\text{M} + \text{Na}^+$) and 631.35 ($\text{M} + \text{K}^+$). IR (KBr): 1650(s) (C = O), 1610, 1485, 1295, 1201, 1114, 1007, 923, 884 cm^{-1} . ^1H NMR (300 Hz, CDCl_3): δ (ppm) 1.31 [s, 18H, $\text{C}(\text{CH}_3)_3$]; 2.16 [s, 6H, OCH_3]; 3.75 [br s, 8H, ArCH_2Ar]; 6.29 [s, 4H, QuH]; 7.19 [s, 4H, ArH].

Results and discussion

Voltammetric studies

The electrochemical behaviour of **1** was investigated by cyclic voltammetry, square wave voltammetry and rotating-disk voltammetry at platinum electrode in CH_3CN –0.1 M TBAP.

Figure 1 shows the cyclic voltammogram of **1** at 100 mVs^{-1} . Four main oxidation peaks were detected. The first

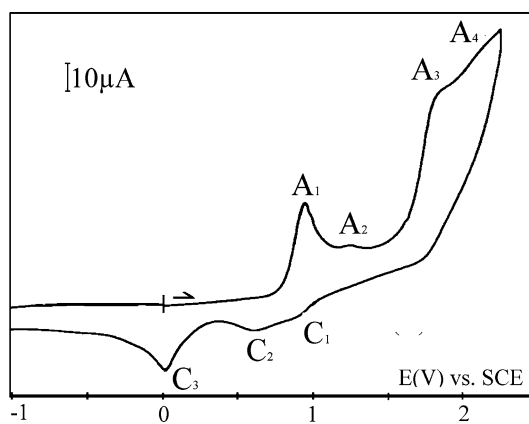


Fig. 1 Cyclic voltammogram at Pt disk electrode ($\Phi = 2\text{ mm}$) of 1.44 mM **1** in $\text{CH}_3\text{CN} + 0.1\text{ M TBAP}$. Sweep rate: 100 mV s^{-1}

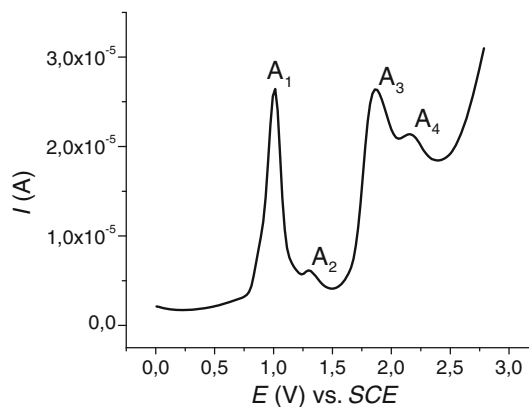


Fig. 2 SWV response of the Pt electrode in 1.95 mM **1** ($\text{CH}_3\text{CN} + 0.1\text{ M TBAP}$). $a = 25\text{ mV}$; $\Delta E_S = 20\text{ mV}$; $f = 10\text{ s}^{-1}$. Curve corresponding to the anodic scan

anodic peak (A_1) was observed at 0.94 V. A small oxidation peak (A_2) appears at 1.23 V. In the potential range between 1.8 and 2.2 V, two overlapped waves (A_3 and A_4) were noticed. In reverse direction, two small and irreversible cathodic waves (C_1 and C_2) were observed at 0.89 and 0.62 V, respectively. At 0.00 V, a well-defined and irreversible peak C_3 appears.

SWV (Fig. 2) confirmed the electroactivity of **1** obtained in the potential range 0.3–2.4 V. In fact, four redox processes were observed at 1.01, 1.31, 1.86 and 2.18 V, respectively. The height of the first and the third (A_1 and A_3) peak was similar. However, they show that the number of electrons displayed are similar too.

Figure 3 reported the cyclic voltammograms of **1** evolution with scan rates. It was evident that for $v \geq 50\text{ mV s}^{-1}$ a cathodic peak (C_3) (Fig. 3, curves c, d and e) centered at ca. 0.00 V with a current maximum of $I_{\text{max}} = 86\text{ μA}$ (scan rate: 500 mVs^{-1}) was detected.

The repetitive CV in the aprotic media was examined and does not show passivation of the electrode. However,

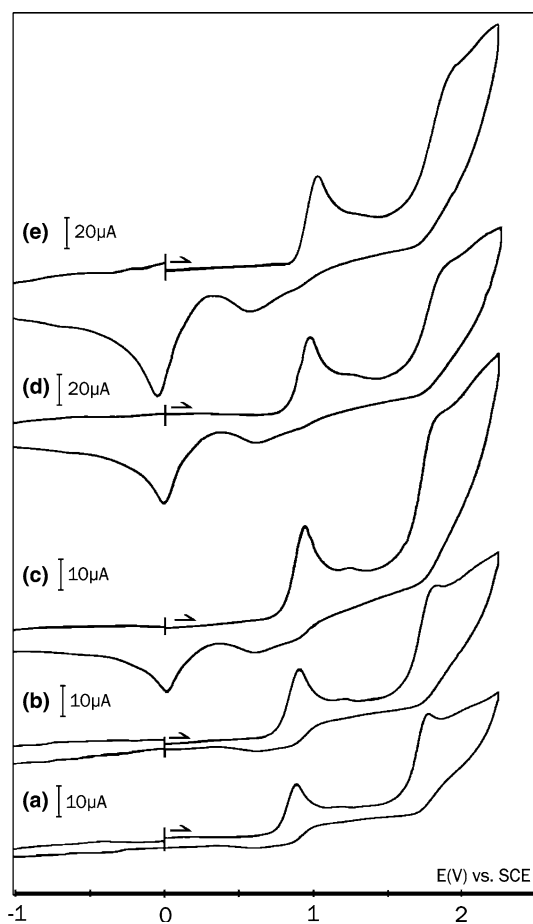


Fig. 3 Cyclic voltammogram at Pt disk electrode ($\Phi = 2$ mm) at various scan rates of 1.44 mM **1** in $\text{CH}_3\text{CN} + 0.1$ M TBAP. Sweep rates from (a) to (e) were: 25, 50, 100, 250, 500 mV s^{-1}

this result was in good agreement with that reported in the literature for different phenolic derivatives and is usually associated with various chemical reactions leading to different oxidation products (dimerization products, quinones derivatives) that do not necessarily passivate the electrode surface [25, 26].

Based on the two-electron character of the oxidation wave, it was proposed that the electrochemical oxidation of hydroquinone in acetonitrile consists in a sequence of two electrons and one proton transfer reactions [3]. By comparing the intensity of the first peak with the reversible system of the ferrocene (Fc^+/Fc) in the same conditions, one electron transfer have been determined for \mathbf{A}_1 . However, \mathbf{A}_1 could be assigned to the formation of a radical monocation of **1** through an irreversible system.

The maximum currents for process \mathbf{A}_1 were measured and plotted as a function of the concentration of **1**. A linear relationship was obtained in the range 0.356–8 mM, in agreement with the Randles-Sevick equation [27].

The plots of the first peak currents versus $v^{1/2}$ and the logarithm of the current versus the logarithm of the

substrate concentration were linear (slope: 0.967 $\mu\text{A}/\text{decade}$) in the sweep rate range 25–500 mV s^{-1} , showing diffusion control process at the electrode [28] and follow the theoretical previsions established by Nicholson and Shain [29].

No evidence for reversibility was seen for the first peak in the range of sweep rates 25–500 mV s^{-1} . It follows from linear plot of the logarithm of the peak current as a function of the logarithm of the sweep rate, that the mass transfer is controlled by diffusion process and the chemical reaction because the slope value of the straight line $\log I_p = f(\log v)$ is equal to 0.426 (≈ 0.5) (Fig. 4).

On the other hand, the increase of the scan rate leads to a shift of the peak potential to anodic value. The slope value of about 30 mV of the linear representation of $E_p = f(\log v)$ illustrated in Fig. 5 [30] and the irreversibility of the first oxidation peak in the range of scan rate allowed in this experiment are in agreement with a fast electron transfer followed by a first-order chemical reaction [31]. In addition, the peak potential shifts positively by about 30 mV per decade of the substrate concentration (Fig. 6). In our point of view and according to the literature, this chemical reaction is probably the deprotonation reaction of the cation radical emerging from the first electron transfer.

Figure 7 depicts the voltammogram of **1** which was obtained at a rotating platinum-disk electrode in the supporting electrolyte in the potential range 0–2.5 V; compound **1** exhibits two oxidation process. The first wave shows a clear potential-independent plateau. The plots of E versus $\omega^{1/2}$ (ω : rotating-disk rate) in a first time and E versus $\log(I/I_L - I)$ in a second time resulted in a straight line with a slope of 63 mV per decade. The slope was in agreement with the value of 58 mV for a reversible one-electron transfer [32]. From the slopes, the value of the diffusion coefficient of **1** in acetonitrile was obtained: $D = 3.07 \times 10^{-5} \text{ cm}^2 \text{s}^{-1}$. Moreover, the standard potential was calculated: $E = 1.06$ V.

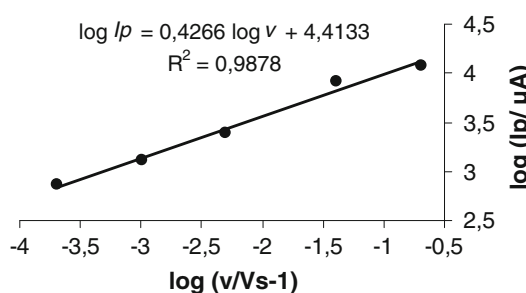


Fig. 4 Variation of the logarithm of the first peak current of **1** in $\text{CH}_3\text{CN} + 0.1$ M TBAP as a function of the logarithm of the sweep rate. Platinum electrode ($\Phi = 2$ mm), reference SCE. Concentration 144 mM

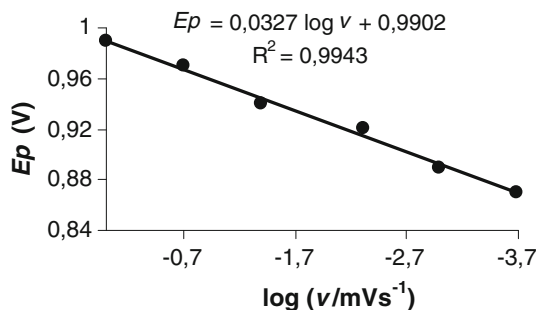


Fig. 5 Variation of the oxidation peak potential of **1** in $\text{CH}_3\text{CN} + 0.1 \text{ M TBAP}$ as a function of the logarithm of the sweep rate. Platinum electrode ($\Phi = 2 \text{ mm}$), reference SCE. Concentration 144 mM

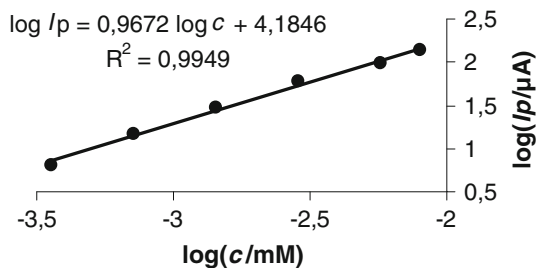


Fig. 6 Variation of the logarithm of the first peak current of **1** in $\text{CH}_3\text{CN} + 0.1 \text{ M TBAP}$ as a function of the logarithm of substrate concentration. Platinum electrode ($\Phi = 2 \text{ mm}$), reference SCE. Sweep rate $v = 100 \text{ mV s}^{-1}$

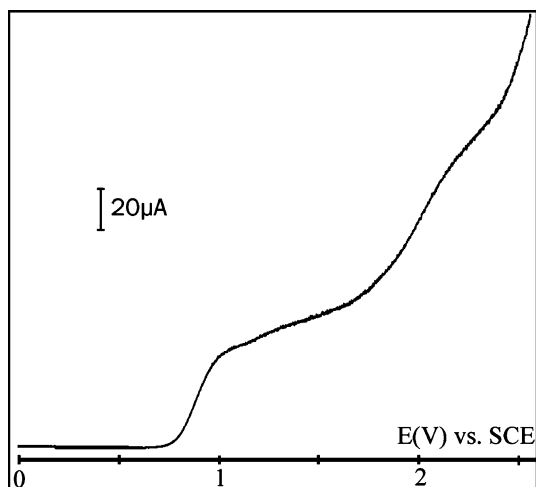


Fig. 7 Rotating disk voltammogram of **1** in $\text{CH}_3\text{CN} + 0.1 \text{ M TBAP}$. Platinum electrode ($\Phi = 2 \text{ mm}$), reference SCE. Concentration 1,44 mM (rotation rate 800 rev min^{-1})

Cyclic voltammograms obtained by changing the potential range were illustrated in Fig. 8. When the first anodic wave A_1 is observed separately over a short potential range (-0.2 to 1.12 V), (Fig. 8, curve a) the classic CV of the hydroquinone in acetonitrile solution were obtained [20]. It shows that to the anodic wave A_1

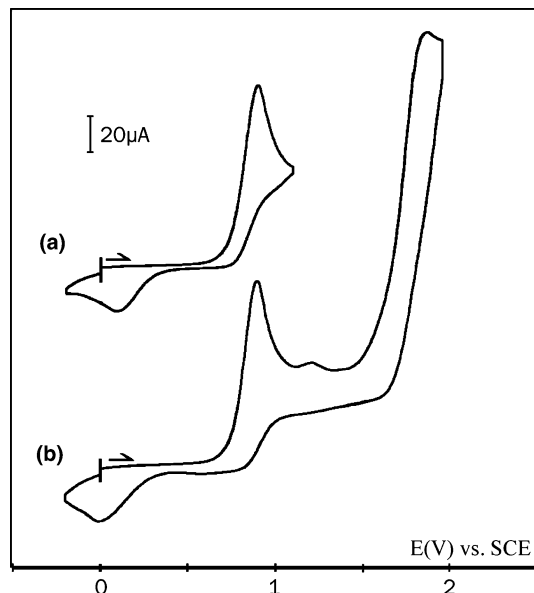


Fig. 8 Cyclic voltammogram at Pt disk electrode ($\Phi = 2 \text{ mm}$) at several potential range of $8 \times 10^{-3} \text{ M } \mathbf{1}$ in $\text{CH}_3\text{CN} + 0.1 \text{ M TBAP}$. $v = 100 \text{ mV s}^{-1}$. Potential range: *a* -0.2 to 1.12 V ; *b* -0.2 to 1.99 V

corresponds a cathodic peak C_3 through an irreversible system ($\Delta E_p (A_1/C_3) = 0.94 \text{ V}$). It could be assigned to the monoprotonated quinone [4]. The first anodic peak A_1 shifts slightly towards the highest potential value when the potential range decreases, the cathodic peak C_3 as well. When the potential range was switched at 1.99 V (Fig. 8 curve b), the cathodic peaks C_1 and C_2 disappear.

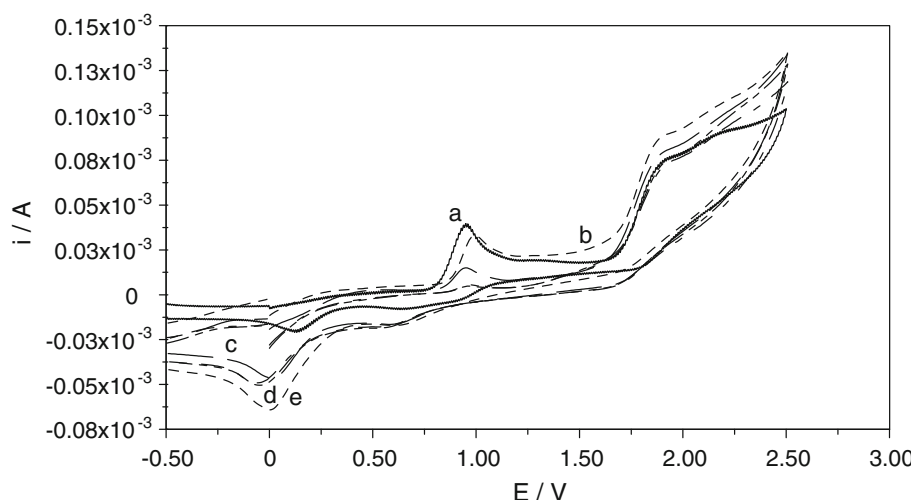
Chronoamperometry

Bulk electrolysis of **1** (46.5 mg; 0.078 mmol) was accomplished at a potential slightly more anodic than the first anodic wave (1.3 V). Homogenization of the electrolytic solution was ensured by a mechanical stirring.

The cyclic voltammetry applied for the substrate explain that the first anodic peak involves only one electron (paragraph 3.1), when we interrupt the electrolysis after consumption of 1 electron per molecule, the corresponding CV (Fig. 9, curve b, time scale of electrolysis: 2 h; $Q_{th} = 7.52 \text{ C}$: Theoretical quantity of coulomb) shows that the first peak intensity value slightly decrease. Two compounds, **2** (10 mg; yield: 21.5%) and **3** (12 mg; yield: 25.8%) were isolated as a pure compounds additionally to the starting material **1** (11 mg; yield: 23, 6%), which were characterized by Maldi-Tof, ^1H NMR and ATR IR spectrometric analyses (structure defined in the “Experimental” section). Product **2** was slightly yellowish and presents an intermediate product which forms during the electrolysis, **3** is an intense yellow powder and could be the majority product.

The total electrolysis was stopped when the level of intensity became sufficiently low, required a consumption

Fig. 9 Cyclic voltammograms at Pt disk electrode in 1.95 mM **1** in $\text{CH}_3\text{CN} + 0.1 \text{ M TBAP}$. Scan each time scale of 2 h of electrolysis at 1.3 V vs. SCE. Scan rate $v = 100 \text{ mVs}^{-1}$



of 2.25 Faradays per molecule. The solution becomes yellowish. The solvent was removed under vacuum and the oxidation residue mixture was extracted with diethyl ether. The products were separated by chromatography on preparative patches of silica gel with a mixture of dichloromethane-acetone (95/5, v/v). Two products were obtained, the starting substrate **1** and a yellowish product, which corresponds to the calix[4]dquinone **3**, was characterized by ATR IR, ^1H RMN and Maldi-Tof (see link “[Experimental](#)” section). To form the **3** product it is necessary the consumption of 4 electrons per molecule. We observe that, just the amount of 2.25 electrons transfer producing at the electrode surface and the rest of electrons transfer producing in the electrolytic solution to form the resulting product (**3**).

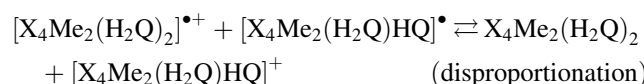
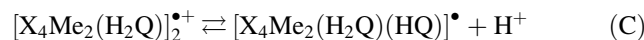
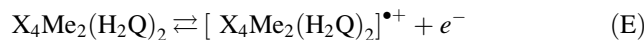
On the other hand, an electrolysis was achieved at 2.1 V (42 mg; 0.07 mmol) subsequent to the third oxidation peak potential (the height wave is approximately equal to one electron) required a consumption of 4.15 Faradays per molecule. This result was in agreement with the number of electron transfer necessary to electrogenerate the final product. The solvent was removed and the residue obtained was extracted with diethyl ether and purified by column chromatography (Silica gel 60, $\text{CH}_2\text{Cl}_2-(\text{CH}_3)_2\text{CO}$, 95/5, v/v). The formed products was purified by chromatography on silica gel with a mixture of dichloromethane-acetone (95/5, v/v) as eluent. Two resulting products were separated, the initial substrate **1** and the product **3**.

Under the experimental conditions, a yellowish product was deposit on the platinum grid. The deposited product on the platinum grill was analysed and it appears that the electrodeposited yellow substance was the calix[4]dquinone **3**.

The macroelectrolysis was controlled by cyclic voltammetry. The voltammograms (Fig. 9) shows that the exhaustive electrooxidation makes the first peak height

very low, but he does not entirely disappear. The bulk electrolysis was controlled by SWV too. Different anodic scans were performed before, during and after electrolysis at 1.3 V. The height of the first peak was decrease as well as the time scale of chronoamperometry increase and becomes almost constant after a time scale of 6 h. This behaviour was similar to that previously observed from CV.

These results indicate that the initial substrate was generating into the oxidation reaction. The situation is of the same type as for a classical ECE-disproportionation mechanism [33]:



The follow-up by cyclic voltammetry and SWV of the chronoamperometry applied at a controlled potential of 2.1 V shows that the first peak height decrease on the first time, later the third peak begin to attenuate.

Nevertheless, after purification, the product **3** was examined by cyclic voltammetry. Figure 10A shows the electroactivity domain of the product. In the potential range of -1.2 to 0 V (Fig. 10B) two reversible reduction processes were obtained (First system: $E_p^{1/2} = -0.675 \text{ V}$; $\Delta E_p = 0.07 \text{ V}$; second system $E_p^{1/2} = -0.815 \text{ V}$; $\Delta E_p = 0.065 \text{ V}$). This result was in agreement with literature [2] and will be present the double reduction of the calix[4]dquinone in acetonitrile media. The product **2** was not examined by CV because the quantity of the isolated product is very small.

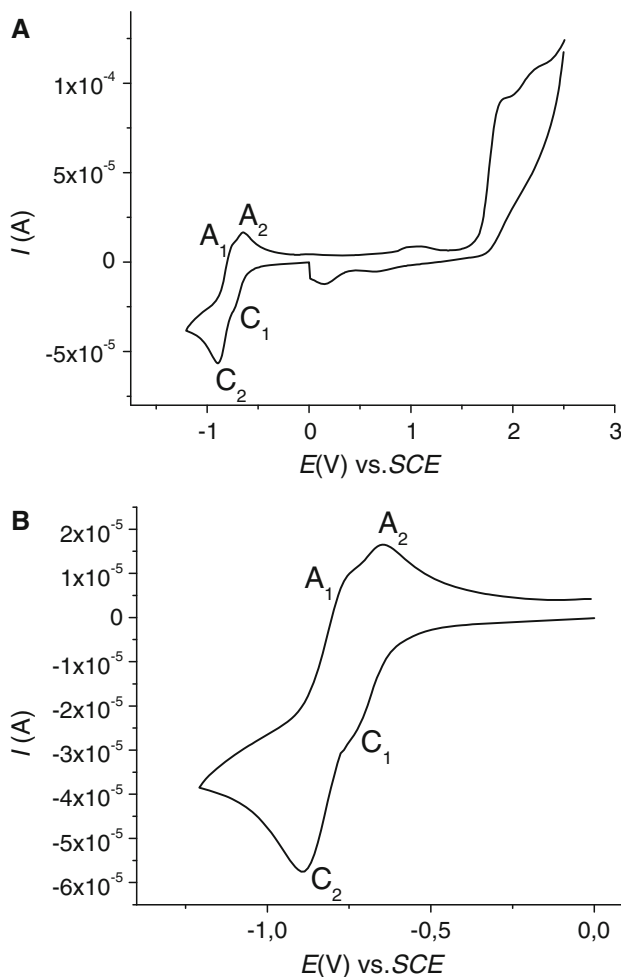


Fig. 10 Cyclic voltammogram at Pt disk electrode of 3.22 mM **3** in $\text{CH}_3\text{CN} + 0.1 \text{ M TBAP}$. **A** Potential range: 0 to -1.2 to 2.5 V ; **B** Zoom of (A), potential range: 0 to -1.2 to 0 V . Platinum electrode ($\phi = 2 \text{ mm}$), reference SCE. Sweep rate $v = 100 \text{ V s}^{-1}$

Voltammetric measurements show that the first electrochemical process A₁ involves an apparent one-electron (n_{app}) [27] transfer mainly produced at the electrode surface. However, this could not be confirmed by coulometric measurements in macroscale electrolysis [9]. On the other hand, cyclic voltammogram obtained at a potential range from -0.2 to 1.31 V , show a new positive/negative peak system at a slightly more positive potential than that of the first oxidation peak. These results clearly indicate the presence of a further electron transfer reaction and also of its coupling with a chemical reaction.

The third anodic step A₃ involves one-electron transfer; it could be assigned to the oxidation of the intermediate product formed in route to generate essentially the final product. Therefore, the first and the second anodic peaks in the cyclic voltammogram may correspond to the oxidation of the first hydroquinone moiety to the monoprotonated quinone moiety. The third and the fourth peaks, may

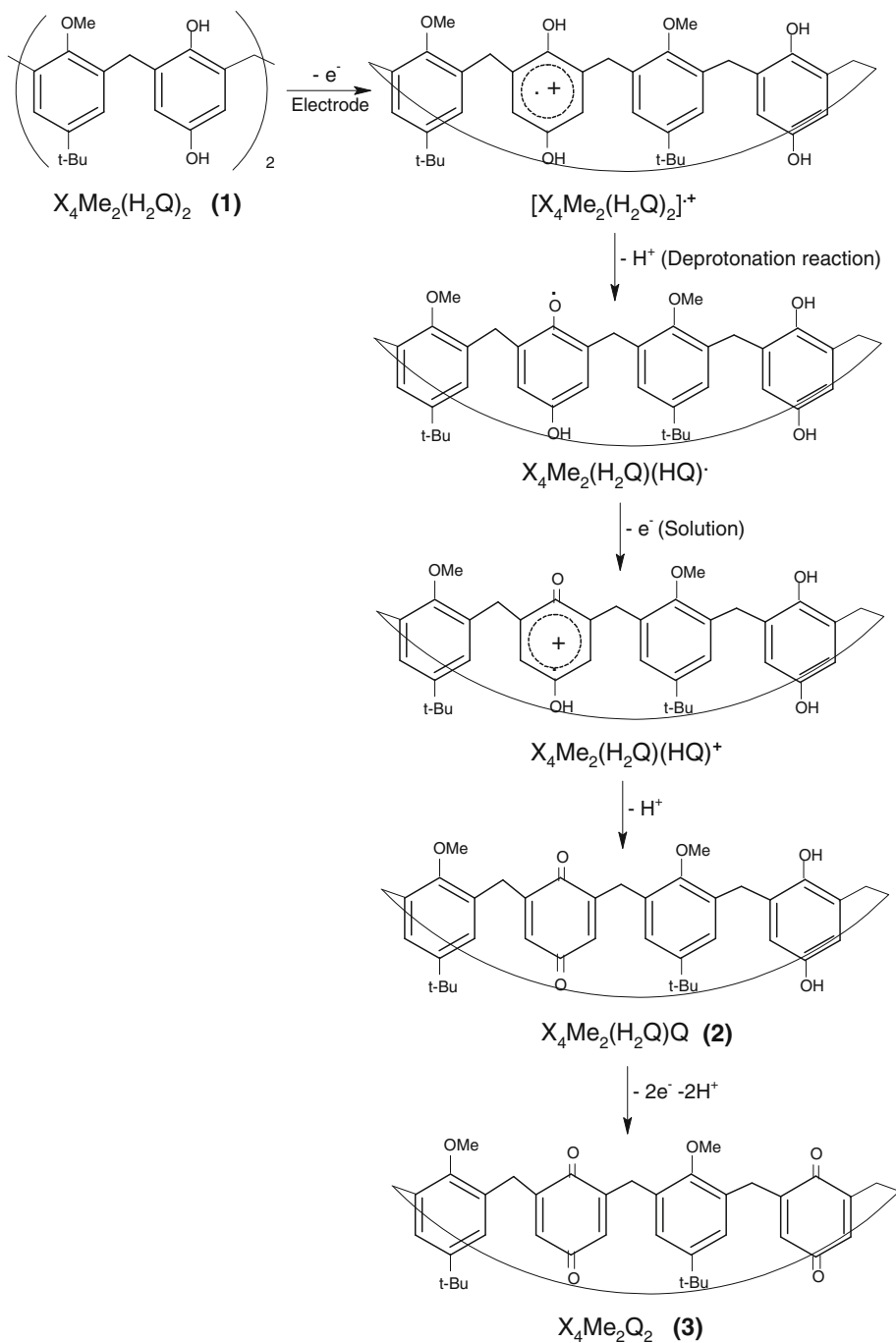
correspond to the oxidation of the next hydroquinone moiety to give the calix[4]arenediquinone. The evolving in solution may follow an ECE sequence [34, 35]. It is generally accepted that the two-electron reduction of $\text{X}_4\text{Me}_2\text{Q}(\text{QH}^+)$ occurs at the level of wave C₃ [36]. The low current intensity of wave C₃ with respect to wave A₁ can be explained by a slow reduction kinetics of $\text{X}_4\text{Me}_2\text{Q}(\text{QH}^+)$, as it is shown by a significant peak potential variation with the scan rate (75 mV/dec).

Taking into account the voltammetric patterns of **1** and **3** and electrolysis results, the detailed mechanism of anodic oxidation of the 5, 17-di-*tert*-butyl-11, 23, 25, 27-di-dihydroxy-26, 28-dimethoxy calix[4]arene is projected in Scheme 2. The mechanism could involve in the first step one-electron transfer (E) which allows the formation to the radical cation **1**^{•+}. The latter undergoes a deprotonation (C_H) to give **1**[•]. The radical undergoes a further electron-transfer reaction in solution. Then, a disproportionation occurs, and generates the departure substrate **1** (see the mechanism of EC_HE-disproportionation). The cationic intermediate $\text{X}_4\text{Me}_2(\text{H}_2\text{Q})(\text{HQ})^+$ undergoes deprotonation to generate a product, which is the calix[4]quinhydron **2**. The rest of the electrochemical and chemical processes occur in the solution. In fact, the literature [37] confirms that the role of electron transfer reactions in solution should be considered as well as electron transfers at the electrode. The calix[4]quinhydron **2** undergoes an EC_HEC_H mechanism, with the loss of two electrons and two protons to generate the foremost product **3**.

Conclusion

In this communication we have shown the oxidative electroactivity using cyclic, square wave and rotating-disk voltammetry. The obtained results show the 5, 17-di-*tert*-butyl-11, 23, 25, 27-di-dihydroxy-26, 28-dimethoxy calix[4]arene exhibit that the first irreversible wave with a mass transfer controlled both by diffusion process and a deprotonation reaction of the cation radical emerging from the charge transfer. The macroscales electrolysis investigated at the first and the third peak potential lead to show that the departure substrate is entirely electrolysed but it was regenerating involving a classical ECE-disproportionation mechanism. The electrochemical generation of the intermediate compound which is the calix[4]quinhydron is followed by the electrosynthesis in solution of the calix[4]diquinone. Thus, we confirm that under conditions of macroelectrolysis requiring long duration experiments, phenolic sites are readily converted into the corresponding quinones. We show too, that when the electrolysis was performed after the third oxidation peak, ($\text{X}_4\text{Me}_2\text{Q}_2$) was

Scheme 2 Schematic pathway from dimethoxycalix[4]arene $X_4\text{Me}_2\text{H}_2$ to the dimethoxycalix[4]arenediquinone $X_4\text{Me}_2\text{Q}_2$ and dimethoxycalix[4]arenedihydroquinone $X_4\text{Me}_2(\text{H}_2\text{Q})_2$



electrogenerated in solution and was deposited afterward, on the platinum grid.

Acknowledgment This work was supported by the Ministry of Scientific Research Technology and Competence Development of Tunisia.

References

- O'Connor, K.M., Arrigan, D.W.M., Svehla, G.: Calixarenes in electroanalysis. *Electroanalysis* **7**(3), 205–215 (1995)
- Chung, T.D., Kim, H.: Electrochemistry of calixarene and its analytical applications. *J. Incl. Phenom. Recognit. Chem.* **32**, 179–193 (1998)
- Suga, K., Fujihira, M., Morita, Y., Agawa, T.: Electrochemical study on calix[4]quinone and calix[4]hydroquinone in N,N-dimethylformamide. *J. Chem. Soc. Faraday Trans.* **87**(10), 1575–1578 (1991)
- Eggins, B.R., Chambers, J.Q.: Proton effects in the electrochemistry of the quinone hydroquinone system in aprotic solvents. *J. Electrochem. Soc.* **117**, 186–191 (1970)
- Morita, Y., Agawa, T., Kai, Y., Kanchisa, N., Kasai, N., Nomura, E., Taniguchi, H.: Conformational control of intramolecular

- electron transfer in Calix[4]dquinones and their cationic complexes. *Chem. Lett.* **1349** (1989)
6. Morita, Y., Agawa, T., Nomura, E., Taniguchi, H.: Syntheses and NMR behavior of calix[4]quinone and calix[4]hydroquinone. *J. Org. Chem.* **57**, 3658 (1992)
 7. Reddy, P.A., Gutsche, C.D.: Calixarenes. 32. Reactions of calix[4]quinines. *J. Org. Chem.* **58**, 3245 (1993)
 8. Reddy, P.A., Kashyap, R.P., Watson, W.M., Gutsche, C.D.: Calixarenes 30. Calixquinones. *Isr. J. Chem.* **32**, 89 (1992)
 9. Vataj, R., Louati, A., Jeunesse, C., Matt, D.: Anodic oxidation of p-Bu(t)-calix[4]arene-(OH)₂ -(OCH₂CONEt₂)₂. Electrogeneration of a calixdquinone in dichloromethane. *Electrochim. Commun.* **2**, 769–775 (2000)
 10. Vataj, R., Ridaoui, H., Louati, A., Gabelica, V., Steyer, S., Matt, D.: First synthesis of a '1,2-dquinone-calix[4]arene'. Interaction of its reduced form with Ag⁺. *J. Electroanal. Chem.* **519**, 123–129 (2002)
 11. Awano, H., Sakai, S., Kuriyama, T., Ohba, Y.: Electrodeposition of quinhydrone. *Synth. Met.* **70**, 1121–1122 (1995)
 12. Sakurai, T.: The crystal structure of the triclinic modification of quinhydrone. *Acta Crystallogr. B*, **19**, 320–329 (1965)
 13. Sakurai, T.: On the refinement of the crystal structures of phe-noquinone and monoclinic quinhydrone. *Acta Crystallogr. B*, **24**, 403–412 (1968)
 14. Regeimbal, J., Gleiter, S., Trumpower, B.L., Yu, C.A., Diwakar, M., Ballou, D.P.: Disulfide bond formation involves a quinhydrone-type charge-transfer complex. *JCA Bardwell, Proc. Natl Acad. Sci. USA* **100**, 13779–13784 (2003)
 15. Gutsche, C.D. (ed): *Calixarenes*. Royal Society of Chemistry, Cambridge (1989)
 16. Beer, P.D., Szemes, F., Passaniti, P., Maestri, M.: Luminescent ruthenium(II) bipyridine-calix[4]arene complexes as receptors for lanthanide cations. *Inorg. Chem.* **43**, 3965–3975 (2004)
 17. Gutsche, C.D., Alam, I.: Calixarenes. 23. the complexation and catalytic properties of water soluble calixarenes. *Tetrahedron* **44**, 4689–4694 (1988)
 18. Sénèque, O., Campion, M., Giorgi, M., Le Mest, Y., Reinaud, O.: Funnel complexes with CoII and NiII: new probes into the biomimetic coordination ability of the calix[6]arene-based tris(imidazole) system. *Eur. J. Inorg. Chem.* 1817–1826 (2004)
 19. Meddeb-Limem, S., Malezieux, B., Herson, P., Besbes-Hentati, S., Said, H., Blais, J.C., Bouvet, M.: The first calixarenequinhydrone: syntheses, self-organized films and solvatochromism. *J. Phys. Org. Chem.* **18**, 1176–1182 (2005)
 20. Astudillo, P.D., Tiburcio, J., Gonzalez, F.J.: The role of acids and bases on the electrochemical oxidation of hydroquinone: hydrogen bonding interactions in acetonitrile. *J. Electroanal. Chem.* **604**, 57–64 (2007)
 21. McKillop, A., Swann, B.P., Taylor, E.C.: Thallium in organic synthesis-XVI. Preparation of p-quinones by oxidation of phenols and hydroquinones with thallium(III) trifluoroacetate. *Tetrahedron* **26**, 4031–4039 (1970)
 22. Van Loon, J.D., Arduini, A., Coppi, L., Verboom, W., Pochini, A., Ungaro, R., Harkema, S., Reinhoudt, D.N.: Selective functionalization of calix[4]arenes at the upper rim. *J. Org. Chem.* **55**, 5639–5646 (1990)
 23. Beer, P.D., Gale, P.A., Chem, Z., Drew, M.G.B., Heath, J.A., Orgden, M.I., Powell, H.R.: New ionophoric calix[4]dquinones: coordination chemistry, electrochemistry, and X-ray crystal structures. *Inorg. Chem.* **36**, 5880–5893 (1997)
 24. Ganjali, S.T., Shafai, M., Khosravi, M.: Simple synthetic strategy to inherently chiral calix[4]arene by an asymmetric calix[4]qui-none as a key intermediate. *Acta Chim. Slov.* **49**, 903–908 (2002)
 25. Webster, R.D.: Voltammetric studies on the α -tocopherol anion and α -tocopheroxyl (Vitamin E) radical in acetonitrile. *Electrochim. Commun.* **1**, 581 (1999)
 26. Richards, J.A., Whiston, P.E., Evans, D.H.: Electrochemical oxidation of 2,4,6-tri-tert-butylphenol. *J. Electroanal. Chem.* **63**, 311 (1975)
 27. Bard, A.J., Faulkner, L.R.: *Electrochemical Methods: Fundamentals and Applications*. Wiley, New York (1980)
 28. Babaei, A., McQuillan, A.J.: An in situ UV-vis and IR spectro-electrochemical study of the deposition of a hydroquinone anion salt on platinum electrodes from dichloromethane solutions. *J. Electroanal. Chem.* **462**, 266–272 (1999)
 29. Nicholson, R.S., Shain, I.: Theory of stationary electrode polarography single scan and cyclic methods applied to reversible, irreversible, and kinetic systems. *J. Anal. Chem.* **36**, 706 (1964)
 30. Simon, P., Farsang, G., Amatore, C.: Mechanistic investigation of the oxidation of p-anisidine in unbuffered DMF using fast scan rates at ultramicroelectrodes. *J. Electroanal. Chem.* **435**, 165 (1997)
 31. Amatore, C., Farsang, G., Maisonneuve, E., Simon, P.: Voltammetric investigation of the anodic dimerization of p-halogeno-anilines in DMF: reactivity of their electrogenerated cation radicals. *J. Electroanal. Chem.* **462**, 55 (1999)
 32. Levich, V.G.: *Physicochemical Hydrodynamics*. Prentice-Hall, Englewood Cliffs (1962)
 33. Andrieux, C.P., Nadjo, L., Savéant, J.M.: Electrodimerization. VII. Electrode and solution electron transfers in the radical-substrate coupling mechanism. Discriminative criteria from the other mechanisms in voltammetric studies (linear sweep, rotating disc, polarography). *J. Electroanal. Chem.* **42**, 223–242 (1973)
 34. Nadjo, L., Savéant, J.M.: Linear sweep voltammetry: kinetic control by charge transfer and/or secondary chemical reactions. I. Formal kinetics. *J. Electroanal. Chem.* **48**, 113 (1973)
 35. Ronlan, A., Parker, V.D.: Anodic oxidation of phenolic compounds. Part II. Products and mechanism of the anodic oxidation of hindered phenols. *J. Chem. Soc. (C)* 3214–3218 (1971)
 36. Macias, N.A., Gonzalez, I., Aguilar-Martinez, M.: Evolution from hydrogen bond to proton transfer pathways in the electro-reduction of α -NH-quinones in acetonitrile. *J. Electrochim. Soc.* **3**, 151 (2004)
 37. Andrieux, C.P., Nadjo, L., Savéant, J.M.: Electrodimerization. I. One-electron irreversible dimerization diagnostic criteria and rate determination procedures for voltammetric studies. *J. Electroanal. Chem.* **26**, 147–186 (1970)